tend to react thermally with iodonium salts, whereas those above the upper limit show reduced efficiency.
16. J. M. Saveant, *J. Chem. Phys.* **92**, 1011 (1988).
17. M. C. Palazotto, M. R. V. Sahyun, N. Serpone, D. K. Sharma, *J. Chem. Phys.* **90**, 3373 (1989).
18. The observed dependence of quantum yield on exposure is inconsistent with exhaustion of reactive, static sites having equal sensitivity. A random distribution of components, together with an inverse exponential dependence of efficiency on separation, can explain the data only if (i) more than one proton is generated per photoevent or (ii) energy transfer allows communication between sites, such that the most efficient sites are exhausted first. The very high initial quantum yields observed (~100% in some cases) cannot otherwise be accounted for.
19. I. R. Gould, D. Ege, J. E. Moser, S. Farid, *J. Am. Chem. Soc.* **112**, 4290 (1990).
20. We acknowledge chemists I. B. K. Bloom, J. J. Cardone, K. Clendening, M. Fitzgerald, R. A. Gaudiana, J. M. Grasshoff, R. W. Haddock, S. Haque, E. S. Kolb, N. S. Lennhoff, C. Lincoln, J. Mack, D. A. McGowan, K. M. Olson, R. H. Pauze, S. M. Ramos, S. E. Rodman, R. S. Shon-Baker, A. A. Silva, S. G. Stroud, J. C. Warner, M. R. Wilson and H. Yang; microscopist H.-R. H. Jen; and physicists A. E. Ames, Y. G. Conturie and W. T. Vetterling for their contributions to this study. We especially thank K. C. Waterman, S. G. Cohen, and C. Steel for their seminal contributions to the acid photogeneration and acid amplification used in this project.

31 May 2002; accepted 25 July 2002
Published online 8 August 2002;
10.1126/science.1074583
Include this information when citing this paper.

Controlled Elimination of Clathrin Heavy-Chain Expression in DT40 Lymphocytes

Frank R. Wettey,[1,2] Steve F. C. Hawkins,[1] Abigail Stewart,[3] J. Paul Luzio,[3] Jonathan C. Howard,[2] Antony P. Jackson[1]*

We exploited the high rate of homologous recombination shown by the chicken B cell line DT40 to inactivate the endogenous alleles for clathrin heavy chain and replace them with human clathrin complementary DNA under the control of a tetracycline-regulatable promoter. Clathrin repression perturbed the activities of Akt-mediated and mitogen-activated protein kinase–mediated signaling pathways and induced apoptosis; this finding suggests that in DT40 cells clathrin helps to maintain the integrity of antiapoptotic survival pathways. We also describe a variant cell line in which these signaling pathways were unaffected by clathrin down-regulation. This variant cell line did not undergo apoptosis in the absence of clathrin and was used to examine the effects of clathrin depletion on membrane-trafficking pathways. Receptor-mediated and fluid-phase endocytosis were both substantially inhibited, and transferrin-receptor recycling was modestly inhibited. Surprisingly, clathrin removal did not affect the morphology or biochemical composition of lysosomes.

Clathrin-coated vesicles play a fundamental role in eukaryotic cells. They internalize selected cell-surface molecules by receptor-mediated endocytosis (RME) and are implicated in the export of lysosomal enzymes from the trans-Golgi network (TGN) (*1, 2*). Targeted gene disruption in single-celled eukaryotes has made an important contribution to the understanding of clathrin function (*3–5*), but this approach is difficult in vertebrate tissue culture cells because of the generally low rate of homologous integration. However, the chicken B cell line DT40 exhibits an exceptionally high rate of homologous recombination and is an increasingly popular tool for gene targeting in vertebrate cells (*6, 7*). We expressed human clathrin cDNA in DT40 cells under the control of a tetracycline-regulatable expression system (Tet-Off) (*8, 9*) and inactivated both endogenous alleles of chicken clathrin heavy-chain. This allowed us to investigate the functional effects of controlled clathrin depletion in a vertebrate context.

Elimination of clathrin heavy-chain expression in DT40 cells induces apoptosis. The amino acid sequence of chicken clathrin heavy chain was 96% identical to its mammalian homolog. DT40 cells have a single clathrin gene per haploid genome. The construction of DT40 cells conditionally deficient in clathrin heavy-chain expression is described in (*10*) (fig. S1, A to C). The initially derived cell line was designated DKO-S. When these cells were grown in the presence of doxycycline, human clathrin expression was repressed within 72 hours to less than 1% of its normal level (Fig. 1A). By 96 hours, clathrin was undetectable. In native DT40 cells, doxycycline had no effect on clathrin expression, cell growth, or the phenotypes investigated in this study (*11*). In DKO-S cells, clathrin repression induced cell death (Fig. 1A). During the course of this work we isolated a variant, designated DKO-R, that remained viable in the absence of clathrin (Fig. 1B). Clathrin depletion in DKO-S cells induced apoptosis, as judged by caspase activation (Fig. 1C) and by the presence of apoptotic bodies and DNA degradation (fig. S2, A and B). Moreover, caspase activity was abolished and DNA degradation was delayed by BOC-Asp-CH_2-FK (BAF), an inhibitor of late-acting caspase-3 isoforms (Fig. 1C) (fig. S2B). In DKO-R cells, caspases were not activated by clathrin removal, but activity was stimulated by the DNA-damaging drug cytosine arabinoside (Fig. 1D). Thus, in DKO-R cells, the apoptotic machinery remained intact but was uncoupled from clathrin-dependent pathways.

DT40 cells are grown in media containing 10% fetal calf serum supplemented with up to 1% chicken serum (*6, 7*). The initial growth of clathrin-expressing DKO-S cells was identical in media supplemented with either 0.25% or 1% chicken serum. However, when clathrin expression was inhibited, cells in 0.25% chicken serum died sooner than cells grown in 1% chicken serum despite identical kinetics of clathrin decline (Fig. 1A). This result suggests that the cells normally require one or more factor(s) from chicken serum for survival, which only become limiting when clathrin expression is reduced. Serum survival factors prevent apoptosis by stimulating receptor-activated signal transduction pathways. One pathway acts via receptor-activated class I phosphatidylinositol 3-kinase, leading to phosphorylation of the serine-threonine kinase Akt. By direct phosphorylation, Akt in turn inactivates proapoptotic proteins containing an Akt recognition sequence (Arg-X-Arg-X-X-Ser/Thr, where X = any amino acid) (*12*). We used immune blotting to detect total and phosphorylated Akt (phospho-Akt). After clathrin depletion, there was a reduction in phospho-Akt (Fig. 2A). To further monitor the activity of the Akt pathway, and without preconceptions about specific downstream targets, we blotted with an antibody raised against a phosphorylated peptide corresponding to the consensus Akt target sequence (*13*). In DT40 cells, this antibody predominantly recognized a 68-kD protein. The class I phosphatidylinositol 3-kinase inhibitor LY294002 reduced the 68-kD signal, whereas activation of the

[1]Department of Biochemistry, University of Cambridge, Building O, Downing Site, Tennis Court Road, Cambridge CB2 1QW, UK. [2]Institute for Genetics, University of Cologne, Zülpicher Strasse 47, D-50674 Cologne, Germany. [3]Department of Clinical Biochemistry and Cambridge Institute for Medical Research, Addenbrooke's Hospital, Hills Road, Cambridge CB2 2XY, UK.

*To whom correspondence should be addressed. E-mail: a.p.jackson@bioc.cam.ac.uk

B cell antigen receptor by antibody cross-linking—a treatment known to stimulate the Akt pathway—enhanced the signal (fig. S3). The antibody to phospho-Akt substrate could thus be used to detect changes in the activity of Akt-mediated pathways. After clathrin depletion in DKO-S cells, the intensity of the 68-kD band was reduced (Fig. 2, A and B). This decline was not a secondary consequence of apoptosis, because it began before caspase activation was apparent (Fig. 2B). We also examined mitogen-activated protein kinase (MAPK) activation after clathrin depletion. The receptor-regulated p42 and p44 MAPKs (ERK1 and ERK2) drive multiple pathways, including mitogenesis and both pro- and antiapoptotic signals (*14*). Antibodies to p42 and p44 MAPK detected a single band of 43 kD. Either a single MAPK isoform is expressed in DT40 cells, or the chicken isoforms overlap in this gel system. (Fig. 2A). In DKO-S cells, clathrin depletion increased MAPK phosphorylation, but again its rise did not occur after caspase activation (Fig. 2, A and B).

In DKO-R cells, the phosphorylation of Akt and MAPK was enhanced relative to that of DKO-S cells, with or without clathrin (Fig. 2A). Note that the intensity of the 68-kD band was unaffected by clathrin depletion (Fig. 2A). This implies a difference in signal pathway regulation compared to DKO-S cells. Their uncoupling from clathrin expression suggests that in DKO-R cells, these pathways could be internally activated downstream of the clathrin-sensitive step, possibly at a shared point in the two pathways. Such internal activation may be expected to render cell survival less dependent on external serum factors; indeed, DKO-R cells were less sensitive than DKO-S cells to serum deprivation (Fig. 2, C and D).

This link between clathrin and apoptosis is consistent with the emerging consensus that there are fundamental connections between membrane-trafficking pathways and signal transduction (*15–17*). We propose that clathrin helps to maintain the intensity of antiapoptotic survival signaling pathways in DT40 cells. Where this occurs is unknown, but an obvious possibility is RME (see below). Ligand-bound receptors are internalized by RME and either degraded in the lysosomes or recycled to the plasma membrane, depending on the particular ligand and receptor (*15*). In rat liver after insulin treatment, phospho-Akt is more active when associated with endosomes than with plasma membrane (*18*). Thus, receptor-bound Akt may need to be internalized for maximum activity, which could explain the suppression of Akt-dependent signaling in DKO-S cells after clathrin depletion.

However, the inhibition of endocytosis may have different consequences on other pathways. A failure to internalize and degrade lysosomally targeted ligand-receptor complexes will increase their lifetime on the plasma membrane, and this in turn may lead to enhanced MAPK activation (*19*). This is consistent with the observed increase in MAPK phosphorylation after clathrin depletion in DKO-S cells. Actively dividing cells normally integrate both mitogenic and survival factor signals via interlocking pathways. If these pathways become unbalanced, cells undergo apoptosis (*20, 21*). The reciprocal perturbation of the MAPK and Akt pathways in clathrin-depleted DKO-S cells may induce such a conflict. Furthermore, the proto-oncogene c-*myc* sensitizes cells to reduced survival factor signaling (*21*), and DT40 cells constitutively express an unusually high level of c-*myc* as a result of their transformation with avian leukosis virus (ALV) (*22*).

Endocytosis and recycling are impaired in clathrin-depleted DKO-R cells. The apoptotic resistance shown by DKO-R cells with respect to clathrin depletion allowed for the study of clathrin function in ways not possible with the original DKO-S line. Clathrin-expressing cells contained many coated pits. These were missing in the absence of clathrin (Fig. 3, A to C). DT40 cells shed ALV into the medium (*22*), and virus particles were prominent both with and without clathrin. In clathrin-expressing cells, ALV particles were often associated with coated pits (Fig. 3A) and with internal membrane-bound compartments (Fig. 3B). Without clathrin, these internal structures disappeared and viruses accumulated on the extracellular surface (Fig. 3C), demonstrating that ALV enters cells primarily via clathrin-coated pits. We measured the internalization of ^{125}I-labeled conalbumin, the chicken egg white isoform of transferrin. In clathrin-expressing cells, ligand accumulation was rapid. DT40 is a fast-growing cell line (*7*) and may require a high endocytic capacity. In the complete absence of clathrin, the initial rate of uptake was reduced by a factor of nearly 6 (Fig. 3D). This is similar to the effect on RME of dominant-negative mutants of clathrin (*23*) and of other coated pit components such as dynamin (*24*) and Eps15 (*25*). Clathrin removal also inhibited fluid-phase uptake of horseradish peroxidase (HRP) to about the same degree (Fig. 3E). This is consistent with experiments in which microinjected antibodies to clathrin inhibited both RME and fluid-phase endocytosis (*26*). But in the present example, the ability to effectively repress clathrin expression in DKO-R cells unambiguously revealed

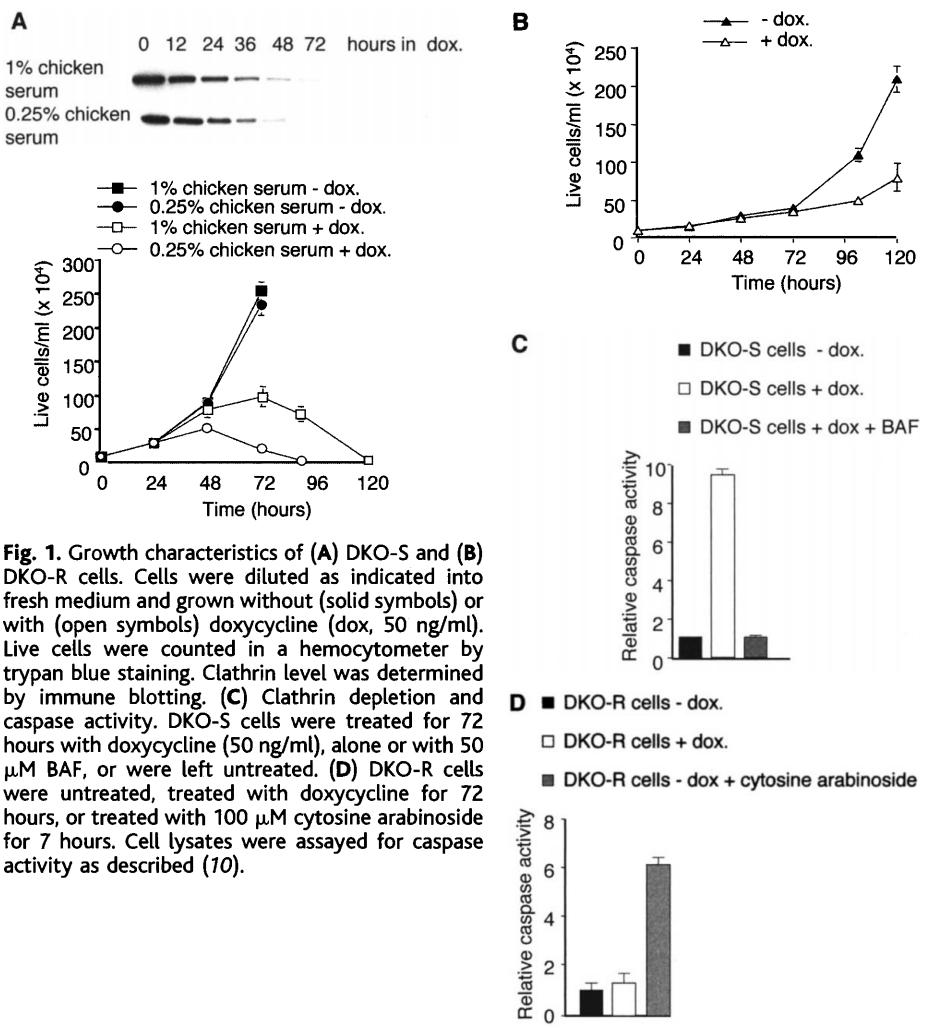

Fig. 1. Growth characteristics of (**A**) DKO-S and (**B**) DKO-R cells. Cells were diluted as indicated into fresh medium and grown without (solid symbols) or with (open symbols) doxycycline (dox, 50 ng/ml). Live cells were counted in a hemocytometer by trypan blue staining. Clathrin level was determined by immune blotting. (**C**) Clathrin depletion and caspase activity. DKO-S cells were treated for 72 hours with doxycycline (50 ng/ml), alone or with 50 μM BAF, or were left untreated. (**D**) DKO-R cells were untreated, treated with doxycycline for 72 hours, or treated with 100 μM cytosine arabinoside for 7 hours. Cell lysates were assayed for caspase activity as described (*10*).

the operation of clathrin-independent endocytosis.

We measured the effect of clathrin elimination on transferrin receptor recycling as judged by the reappearance of label into the medium from cells preloaded with ^{125}I-labeled conalbumin. Clathrin elimination reduced both the rate and maximum fraction of conalbumin recycling by 30 to 40% (Fig. 3F).

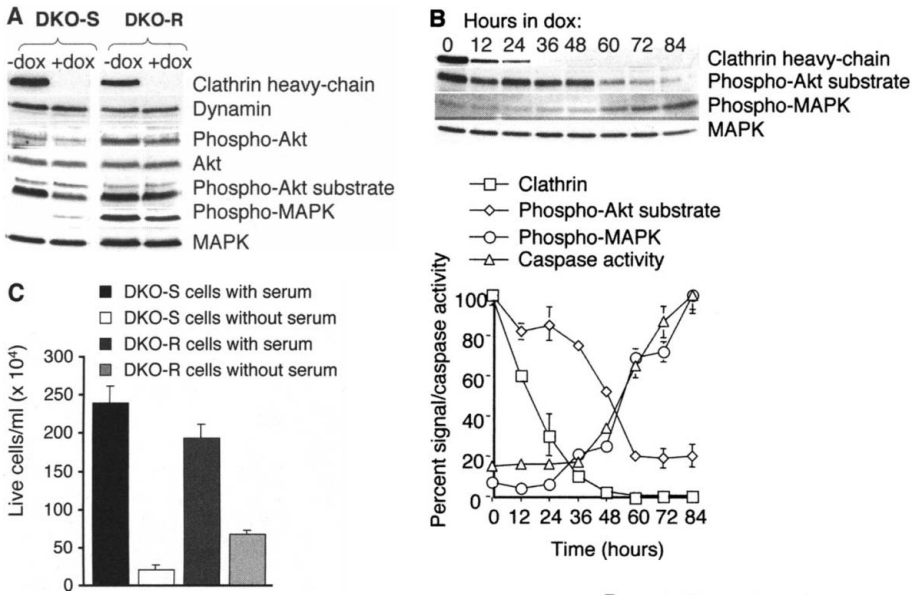

Fig. 2. (**A**) Clathrin depletion and signal pathway activation. Lysates were prepared from DKO-S and DKO-R cells that had been incubated with or without doxycycline (50 ng/ml) for 72 hours. Cell extracts (60 μg) were probed by immune blotting. (**B**) Time course of signaling changes in clathrin-depleted DKO-S cells. DKO-S cells were incubated at 10^6 cells/ml with doxycycline (50 ng/ml) at the start of the experiment. Cells (5×10^6) were harvested at the indicated times; protein levels were monitored by immune blotting and densitometry. For comparison of relative levels, the band intensities and caspase activity are expressed as percentages of their maximum values. (**C** and **D**) Sensitivity of DKO-S and DKO-R cells to serum deprivation. Cells (10^6/ml) were transferred to media with or without serum for 24 hours. Cell viability after this time (C) was determined by trypan blue exclusion. Caspase activity (D) was determined as described (*10*). Values are means ± SE of two experiments performed in triplicate.

Clathrin is found on tubular elements of the early sorting endosome (*27*), where it could help to concentrate recycling receptors. Its absence could lead to receptors diffusing out of the recycling subdomains. This might explain both the reduced fraction and reduced rate of recycling. In contrast to our results, a HeLa cell line expressing a dominant-negative clathrin mutant showed only a minimal effect on recycling (*23*). These differences could hint at the presence of multiple recycling paths in different cells.

Adaptor distribution in clathrin-depleted DKO-R cells. We examined the distribution of GGA1, γ-adaptin (AP1), α-adaptin (AP2), and δ-adaptin (AP3) adaptors in cells with and without clathrin; together, these represent most adaptor classes associated with clathrin-coated vesicles (*2*). In cells expressing clathrin, both GGA1 and AP1 were localized to a perinuclear area consistent with the TGN (Fig. 4, C and E). AP2 was localized in a punctate pattern (Fig. 4G), and AP3 stained vesicular cytosolic structures that were distinct from the AP1 and AP2 stains (Fig. 4I). Without clathrin, the adaptors remained associated with their target membranes (Fig. 4, D, F, H, and J), which confirms that efficient adaptor targeting does not require clathrin. For GGA1 and AP1 in particular, the staining was strikingly enhanced (Fig. 4, D and F). The reason is unclear. As judged by immune blotting, the levels of AP1 and GGA1 did not change after clathrin depletion (*11*). It is possible that clathrin removal further exposed antibody epitopes, but this seems unlikely because we consistently found the same phenomenon for AP1 and GGA1 using different antibodies raised against distinct epitopes (*11*). Alternatively, the absence of clathrin may impair

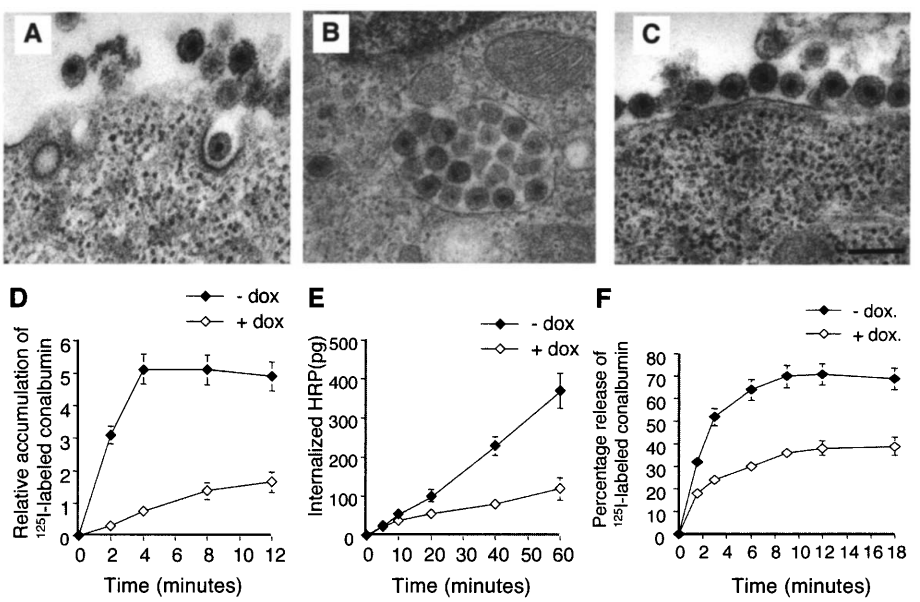

Fig. 3. Transmission electron microscopy (TEM) images of DKO-R cells grown either without (**A** and **B**) or with (**C**) doxycycline (50 ng/ml) for 96 hours. (A) Coated pits with ALV particles. (B) Internal membrane compartments containing mature ALV. (C) ALV accumulation on the cell surface in the absence of coated pits. Scale bar, 200 nm. (**D**) Clathrin depletion and RME. Exponentially growing cells were grown with or without doxycycline (50 ng/ml) for 96 hours. The internalization of prebound ^{125}I-labeled conalbumin in the continuous presence of label was followed for the indicated times (*10*). Data points are means ± SE of the experiments performed in triplicate. (**E**) Fluid-phase endocytosis of HRP in DKO-R cells either untreated or treated with doxycycline (50 ng/ml) for 96 hours. Internalized label was assayed as described (*10*). Data points are means ± SE of experiments performed in triplicate. (**F**) Conalbumin recycling. Exponentially growing cells were incubated with or without doxycycline (50 ng/ml) for 96 hours and preloaded with ^{125}I-labeled conalbumin (*10*). Data points (means ± SE of two experiments performed in triplicate) record the appearance of label into fresh media. Clathrin elimination was confirmed by Western blotting.

adaptor detachment, leading to adaptor accumulation, but this will require further work to confirm. AP2 adaptors relocalized to the plasma membrane in the absence of clathrin, often forming a continuous ring around the cell (Fig. 4H). AP2 adaptors can form lateral associations (*28*); without clathrin to induce local curvature, these may become dominant, producing a more extended pattern.

Clathrin-independent lysosome biogenesis in DKO-R cells. Surprisingly, clathrin removal did not lead to increased secretion of the lysosomal hydrolase β-glucuronidase (Fig. 5A). When the subcellular distribution of β-glucuronidase was examined by Percoll gradient fractionation, enzyme activity was separated into two peaks. One was associated with the densest fraction, characteristic of mature dense-core lysosomes. The lighter peak may represent late endocytic vesicles. A similar pattern was observed in Percoll-fractionated organelles from *Dictyostelium discoideum* (*5*). Clathrin depletion had no effect on the steady-state distribution of β-glucuronidase between the two peaks (Fig. 5B).

Colloidal conjugates of bovine serum albumin (BSA) and gold are taken into cells through fluid-phase endocytosis and accumulate in dense-core lysosomes (*29*). We used this technique to examine lysosome morphology in the presence and absence of clathrin. In both situations, label accumulated in electron-dense organelles (Fig. 5, C and D). These structures stained positive for LEP100, an avian glycoprotein belonging to the LAMP-1 family of integral lysosomal membrane proteins (*30*) (Fig. 5, E and F). As judged by immunofluorescence staining, the overall cellular distribution of LEP100 was unaffected by clathrin depletion (fig. S4). Within the lysosomes, the accumulated BSA-gold particles were flocculated, indicating that they had undergone proteolysis (*29*).

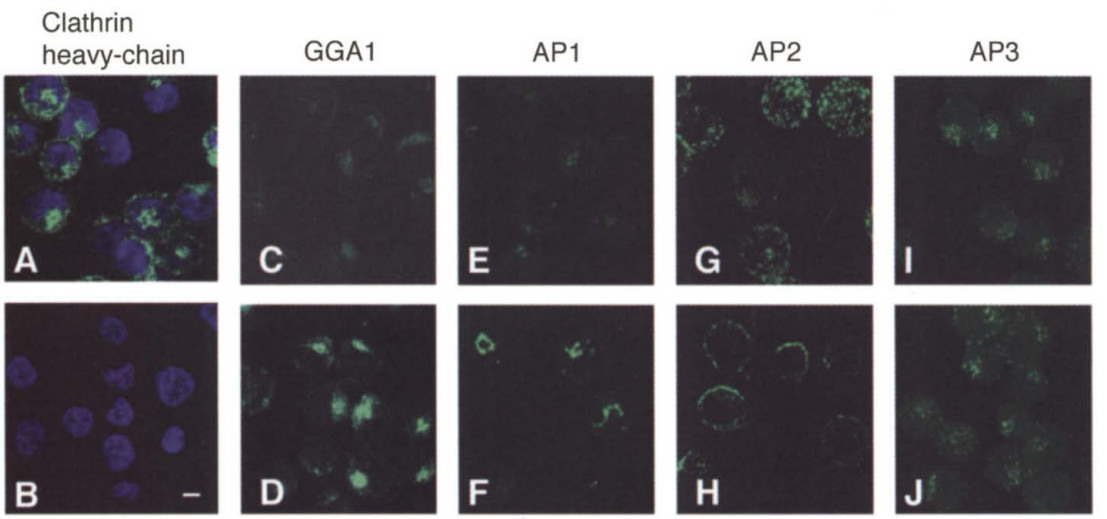

Fig. 4. Confocal immunofluorescence microscopy analysis of adaptor distribution in DKO-R cells grown without (**A**, **C**, **E**, **G**, and **I**) or with (**B**, **D**, **F**, **H**, and **J**) doxycycline (50 ng/ml) for 96 hours. In (A) and (B), nuclei were stained with Hoechst 33342. Scale bar, 5 μm.

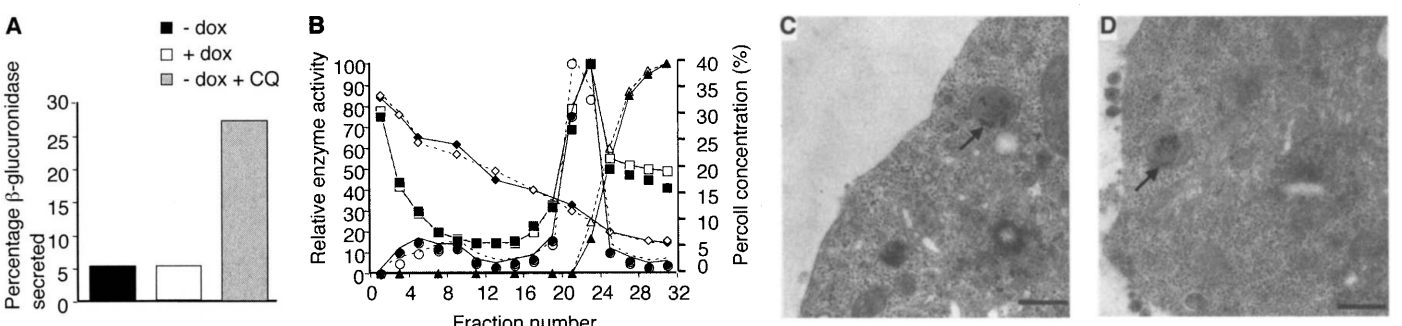

Fig. 5. (**A**) Secretion of β-glucuronidase from cells after growth for 72 hours without or with doxycycline (50 ng/ml) and from cells treated with chloroquine (CQ). Points are means of a representative experiment performed in triplicate. (**B**) Organelle fractionation of DKO-R cells. Cells grown for 96 hours without (solid symbols) or with (open symbols) doxycycline (50 ng/ml) were homogenized, and the postnuclear supernatant was fractionated on a 20% Percoll gradient (diamonds) (*10*). Fractions were collected from the bottom (= 1) and analyzed for the enzyme activities indicated (β-glucuronidase, squares; galactosyltransferase, circles; lactate dehydrogenase, triangles). (**C** and **D**) Lysosomes from cells after growth for 96 hours without (C) or with (D) doxycycline (50 ng/ml). Cells were pulsed with conjugates of BSA and 5-nm colloidal gold for 4 hours, chased for 20 hours to label lysosomes, and prepared for routine TEM as described (*10*). Flocculated gold particles (arrows) are present in electron-dense organelles characteristic of lysosomes. Note the presence of viral particles at the plasma membrane of cells lacking clathrin. Scale bars, 200 nm. (**E** and **F**) Ultrathin cryosections of cells with lysosomes labeled as in (C) and (D), grown for 96 hours without (E) or with (F) doxycycline (50 ng/ml). The sections were stained with LEP100 mAb followed by goat antibody to mouse IgG conjugated to 10-nm colloidal gold. Scale bars, 200 nm. (**G**) Area profile of lysosomes randomly chosen from routine TEM images of cells grown without (solid bars) and with (open bars) doxycycline (50 ng/ml) for 96 hours. Clathrin elimination was confirmed by immune blotting.

Thus, lysosomes from clathrin-depleted cells are functional. There was no clear difference in the lysosome area profile between cells with and without clathrin (Fig. 5G).

Our data indicate that DKO-R cells express a combined pathway of lysosome biogenesis and turnover that does not show an obligatory dependence on clathrin. It is possible that the DKO-R cell line up-regulated clathrin-independent pathways during the time taken to suppress clathrin expression. Yeast cells expressing a temperature-sensitive clathrin mutant compensate for clathrin inactivation after several hours at the nonpermissive temperature (*31*). But in principle, this question can now be addressed by introducing a similar temperature-sensitive clathrin mutant into DKO-R cells. On the other hand, there is evidence for the existence of alternative pathways of lysosome biogenesis that are present in distinct cell types. For example, LAMP-1 is transported to lysosomes by an AP3-dependent but clathrin-independent mechanism (*32*). The successful targeting of LEP100 in clathrin-depleted DKO-R cells is consistent with this finding. Moreover, lymphocytes and lymphocyte-derived cell lines that lack mannose 6-phosphate receptors (M6PRs) nonetheless retain functional lysosomes (*33, 34*), suggesting that lymphocytes contain an M6PR-independent pathway of lysosome biogenesis. Because DT40 is a lymphocyte cell line, it probably expresses this pathway. If so, the pathway may also be clathrin-independent.

Dense-core lysosomes repeatedly fuse with late endosomes and reform after selective membrane retrieval (*35*). Clathrin has been detected on mammalian lysosomal membranes in vitro, and it has been proposed that clathrin-coated vesicles play a central role in lysosome fusion and recycling (*36*). However, our results can only be reconciled with this view if a reduced recycling rate out of the lysosome caused by clathrin loss is balanced by an exactly proportional reduction in biosynthesis. Clearly, it will now be important to examine the turnover kinetics of individual lysosomal proteins with and without clathrin. But even if clathrin does play a role, it cannot be essential. Our results raise important and unexpected questions about clathrin function, and we have produced flexible experimental models that will enable us to address these issues in cells without interference from endogenous clathrin expression.

References and Notes

1. S. L. Schmid, *Annu. Rev. Biochem.* **66**, 511 (1997).
2. F. M. Brodsky, C.-Y. Chen, C. Knuehl, M. C. Towler, D. E. Wakeham, *Annu. Rev. Cell Dev. Biol.* **17**, 517 (2001).
3. S. K. Lemmon, E. W. Jones, *Science* **238**, 504 (1987).
4. G. S. Payne, T. B. Hasson, M. S. Hasson, R. Schekman, *Mol. Cell. Biol.* **7**, 3888 (1987).
5. T. Ruscetti, J. A. Cardelli, M. L. Niswonger, T. J. O'Halloran, *J. Cell Biol.* **126**, 343 (1994).
6. J.-M. Buerstedde, S. Takeda, *Cell* **67**, 179 (1991).
7. P. Winding, M. W. Berchtold, *J. Immunol. Methods* **249**, 1 (2001).
8. M. Gossen, H. Bujard, *Proc. Natl. Acad. Sci. U.S.A.* **89**, 5547 (1992).
9. E. Sonoda *et al.*, *EMBO J.* **17**, 598 (1998).
10. See supporting data on *Science* Online.
11. F. R. Wettey, data not shown.
12. D. P. Brazil, B. A. Hemmings, *Trends Biochem. Sci.* **26**, 657 (2001).
13. J. Jin *et al.*, *Dev. Cell* **1**, 817 (2001).
14. H. J. Schaeffer, M. J. Weber, *Mol. Cell. Biol.* **19**, 2435 (1999).
15. P. C. Baass, G. M. Di Guglielmo, F. Authier, B. I. Posner, J. J. M. Bergeron, *Trends Cell Biol.* **5**, 465 (1995).
16. G. Carpenter, *Bioessays* **22**, 697 (2000).
17. B. P. Ceresa, S. L. Schmid, *Curr. Opin. Cell Biol.* **12**, 204 (2000).
18. A. Balbis, G. Baquiran, J. J. M. Bergeron, B. I. Posner, *Endocrinology* **141**, 4041 (2000).
19. M. Babst, G. Odorizzi, E. J. Estepa, S. D. Emr, *Traffic* **1**, 248 (2000).
20. G. Evan, T. Littlewood, *Science* **281**, 1317 (1998).
21. A.-O. Hueber, G. Evan, *Trends Genet.* **14**, 364 (1998).
22. T. W. Baba, B. P. Giroir, E. H. Humphries, *Virology* **144**, 139 (1985).
23. E. M. Bennett, S. X. Lin, M. C. Towler, F. R. Maxfield, F. M. Brodsky, *Mol. Biol. Cell* **12**, 2790 (2001).
24. H. Damke, T. Baba, D. E. Warnock, S. L. Schmid, *J. Cell Biol.* **127**, 915 (1994).
25. A. Benmerah *et al.*, *J. Cell Biol.* **140**, 1055 (1998).
26. S. J. Doxsey, F. M. Brodsky, G. S. Blank, A. Helenius, *Cell* **50**, 453 (1987).
27. E. M. van Dam, W. Stoorvogel, *Mol. Biol. Cell* **13**, 169 (2002).
28. M. P. Chang, W. G. Mallet, K. E. Mostov, F. M. Brodsky, *EMBO J.* **12**, 2169 (1993).
29. N. A. Bright, B. J. Reaves, B. M. Mullock, J. P. Luzio, *J. Cell Sci.* **110**, 2027 (1997).
30. J. Lippincott-Schwartz, D. M. Fambrough, *Cell* **49**, 669 (1987).
31. M. Seeger, G. S. Payne, *EMBO J.* **11**, 2811 (1992).
32. A. A. Peden, R. E. Rudge, W. W. Y. Lui, M. S. Robinson, *J. Cell Biol.* **156**, 327 (2002).
33. C. A. Gabel, S. Kornfeld, *J. Cell Biol.* **99**, 296 (1984).
34. F. Dittmer *et al.*, *J. Cell Sci.* **112**, 1591 (1999).
35. J. P. Luzio *et al.*, *J. Cell Sci.* **113**, 1515 (2000).
36. L. M. Traub *et al.*, *J. Cell Biol.* **135**, 1801 (1996).

37. We thank H. Bujard for rtTA vector; T. Nagase for human clathrin heavy-chain cDNA; B. Malissen for plasmid encoding L-histidinol resistance; J. Ortin for plasmid pBSpacΔp encoding puromycin resistance; M. Takata for plasmids containing neomycin- and hygromycin-resistance cassettes; F. M. Brodsky for clathrin heavy-chain monoclonal antibodies (mAbs) X22 for immunofluorescence and TD.1 for blotting; M. S. Robinson for antibodies to γ-adaptin (AP1), α-adaptin (AP2), and D. M. Fambrough for LEP100 mAb. Antibodies to p42/p44 MAPK (MK12) and dynamin were obtained from Transduction Laboratories. Antibodies to Akt, phospho-Akt (Ser^{473}), phospho-Akt substrate, and phospho-p42/44 MAPK (Thr^{202}/Tyr^{204}) were from Cell Signalling Technology, L. Sellers, and A. Tolkovsky. Goat antibody to mouse immunoglobulin G (IgG) conjugated to 10-nm colloidal gold was from British Biocell. HRP- and dye-conjugated antibodies to rabbit and mouse IgG were from Bio-Rad and Molecular Probes, respectively. We thank D. F. Cutler, H. Davidson, M. S. Robinson, P. Shepherd, and A. M. Tolkovsky for helpful discussion and comments on the manuscript and C. Boucher, H. Chatwin, and S. Dornan for help with genomic analysis. Supported by grants from the Biotechnology and Biological Sciences Research Council and the Wellcome Trust (A.P.J. and J.C.H.), the Royal Society (A.P.J.), Deutsche Forschungsgemeinschaft (SFB 243 and 274) and Land Nordrhein-Westfalen through the University of Cologne (J.C.H.), the Medical Research Council (J.P.L), and a predoctoral Marie Curie Fellowship from the European Commission (F.R.W.). The partial cDNA sequence of chicken clathrin heavy chain has been submitted to the EMBL database under accession number AJ427965. Partial genomic sequences have been submitted to the EMBL database under accession numbers AJ429072, AJ429073, AJ429074, AJ429075, and AJ429076.

Supporting Online Material

www.sciencemag.org/cgi/content/full/297/5586/1521/DC1

Materials and Methods

Figs. S1 to S4

22 May 2002; accepted 18 July 2002

SynCAM, a Synaptic Adhesion Molecule That Drives Synapse Assembly

Thomas Biederer,[1]* Yildirim Sara,[1] Marina Mozhayeva,[1] Deniz Atasoy,[1] Xinran Liu,[1,2] Ege T. Kavalali,[1,3] Thomas C. Südhof[1,2,4]*

Synapses, the junctions between nerve cells through which they communicate, are formed by the coordinated assembly and tight attachment of pre- and postsynaptic specializations. We now show that SynCAM is a brain-specific, immunoglobulin domain–containing protein that binds to intracellular PDZ-domain proteins and functions as a homophilic cell adhesion molecule at the synapse. Expression of the isolated cytoplasmic tail of SynCAM in neurons inhibited synapse assembly. Conversely, expression of full-length SynCAM in nonneuronal cells induced synapse formation by cocultured hippocampal neurons with normal release properties. Glutamatergic synaptic transmission was reconstituted in these nonneuronal cells by coexpressing glutamate receptors with SynCAM, which suggests that a single type of adhesion molecule and glutamate receptor are sufficient for a functional postsynaptic response.

Synapses are specialized intercellular junctions that are assembled when an immature presynaptic terminal contacts a postsynaptic cell. At the site of contact, the presynaptic plasma membrane develops into an active zone, which is where synaptic vesicles undergo exocytosis and release neurotransmitters into the synaptic cleft. On the opposite side of the synaptic cleft, the postsynaptic density contains receptors and signaling molecules